J Solid State Electrochem (2010) 14:1807–1811
DOI 10.1007/s10008-010-1115-8

ORIGINAL PAPER

Preparation and characterization of carbon-coated $Li[Ni_{1/3}Co_{1/3}Mn_{1/3}]O_2$ cathode material for lithium-ion batteries

Bin Lin · Zhaoyin Wen · Xiuyan Wang · Yu Liu

Received: 19 November 2009 / Revised: 16 May 2010 / Accepted: 24 May 2010 / Published online: 10 June 2010

Abstract The carbon-coated $Li[Ni_{1/3}Co_{1/3}Mn_{1/3}]O_2$ was synthesized from the porous $Li[Ni_{1/3}Co_{1/3}Mn_{1/3}]O_2$ precursor using citric acid as the carbon source. The electrochemical results showed that both cycling performance and rate capability were improved by the carbon-coating of the $Li[Ni_{1/3}Co_{1/3}Mn_{1/3}]O_2$ materials. It is proposed that the enhanced electrochemical properties by the carbon-coating are attributed to the increased electronic conductivity because the carbon distributed among the surfaces of spherical $Li[Ni_{1/3}Co_{1/3}Mn_{1/3}]O_2$ powders favored the transference of electron and reduced cell polarization.

Keywords Lithium-ion battery · Cathode · $Li[Ni_{1/3}Co_{1/3}Mn_{1/3}]O_2$ · Carbon-coating

Introduction

In recent years, $Li[Ni_{1/3}Co_{1/3}Mn_{1/3}]O_2$ cathode material has been studied widely for use in Li-ion battery to replace the presently popular $LiCoO_2$ [1]. This material has attracted significant interests because the combination of nickel, manganese, and cobalt could provide many advantages such as higher reversible capacity with milder thermal stability at charged state [2], lower cost, and less toxicity than $LiCoO_2$. Thus, $Li[Ni_{1/3}Co_{1/3}Mn_{1/3}]O_2$ might be one of the most promising candidates of cathode material for high-energy, high-power lithium-ion batteries [3].

Despite the positive effect of $Li[Ni_{1/3}Co_{1/3}Mn_{1/3}]O_2$ for the electrochemical property, the delivered capacities have shown a fading while the high rate current density was applied [4]. The addition of dopants [5–8] or the modification of surface [9] of $Li[Ni_{1/3}Co_{1/3}Mn_{1/3}]O_2$ have been studied to improve its performances during cycling at high rate. Many research works confirmed that carbon-coating can enhance electron conductivity to improve the battery's high rate performance [10]. Goodenough et al. [11] have successfully prepared carbon-coated $LiMn_{0.5}Ni_{0.5}O_2$ cathode material and proved the effectiveness of a carbon-coating in increasing the discharge capacity at high current densities and reducing the capacity fade. However, since the preparation of $Li[Ni_{1/3}Co_{1/3}Mn_{1/3}]O_2$ need air atmosphere [1], it is difficult to realize the coating through conventional method in inert atmosphere. In this investigation, based on the porous $Li[Ni_{1/3}Co_{1/3}Mn_{1/3}]O_2$ cathode powders, we filled the pores and coated the surfaces with carbon via the carbonization of citric acid in air and the electrochemical properties were characterized.

Experimental

Sample preparation

$Li[Ni_{1/3}Co_{1/3}Mn_{1/3}]O_2$ was prepared by the slurry spray drying method based the precursors Li_2CO_3, NiO, Co_3O_4, and $MnCO_3$ (all bought from Sinopharm Chemical Reagent Co., Ltd.) as described previously [12]. The spherical and porous cathode materials were obtained after being heated

B. Lin · Z. Wen (✉) · X. Wang · Y. Liu
CAS Key Laboratory of Materials for Energy Conversion,
Shanghai Institute of Ceramics, Chinese Academy of Sciences,
1295 DingXi Road,
Shanghai 200050, People's Republic of China
e-mail: zywen@mail.sic.ac.cn

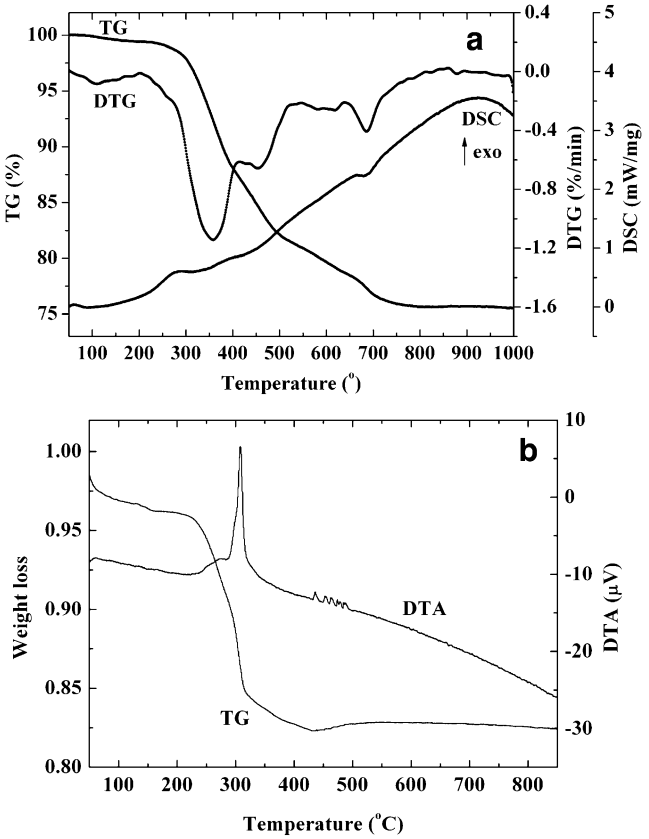

Fig. 1 **a** TG-DTA-DSC curves of the ball-milled precursors (mixture of Li_2CO_3, NiO, Co_3O_4, and $MnCO_3$). **b** TG-DSC curves of the citric acid-LNCMO composite

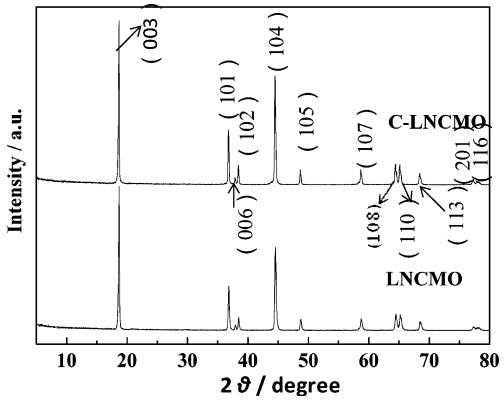

Fig. 3 XRD patterns of the pristine and the carbon-coated $Li[Ni_{1/3}Co_{1/3}Mn_{1/3}]O_2$

at 950 °C for 10 h in air, according to the TG analysis in Fig. 1(a). Carbon-coated $Li[Ni_{1/3}Co_{1/3}Mn_{1/3}]O_2$ was prepared as show in Fig. 2. The citric acid (Sinopharm Chemical Reagent Co., Ltd.) was chosen as carbon source and was first dissolved in ethanol. The $Li[Ni_{1/3}Co_{1/3}Mn_{1/3}]O_2$ particles were then dispersed in the solution. The solution was stirred for 2 h under vacuum environment, allowing the citric acid solution permeate into the pores of $Li[Ni_{1/3}Co_{1/3}Mn_{1/3}]O_2$. After drying, the mixture was calcined at 600 °C for 0.5 h in air to obtain carbon-coated $Li[Ni_{1/3}Co_{1/3}Mn_{1/3}]O_2$. The TG-DTA analysis of the citric acid–$Li[Ni_{1/3}Co_{1/3}Mn_{1/3}]O_2$ was shown in Fig. 1(b).

Characterization

Powder X-ray diffraction (XRD, Rigaku RINT-2000) measurement using Cu Kα radiation was employed to identify the crystalline phase of the synthesized materials. The scan range was 5–80° with a scan step of 0.02° and a scan speed of 10° per min. Scanning electron microscope (SEM, JEOL JSM-6700F) was applied to observe the surface morphology before and after the coating process. The inductively coupled plasma optical emission spectrometry (ICP-OES) was used to determine the chemical composition of the synthesized $LiNi_{1/3}Mn_{1/3}Co_{1/3}O_2$ material. The specific surface area was analyzed by the BET method using a Micromeritics Tristar 3000 in which the N_2 gas adsorption was employed. Each sample was heated at 150 °C for 4 h to remove any adsorbed water before the measurement. The carbon content was measured by thermogravimetric analysis (TGA, NETZSCH 409 PC) from 50–1,000 °C under air with a heating rate of 10 °C/min, and the content was taken as the difference between the relative weight losses exhibited by C-LNCMO and uncoated LNCMO. In order to investigate the nature of the carbon, the Raman spectra were recorded by a Dilor LabRam-1B Raman spectrometer, equipped with a 6.4 mW, 632.8 nm He–Ne laser. The size of the laser beam at the sample was ~0.7 μm.

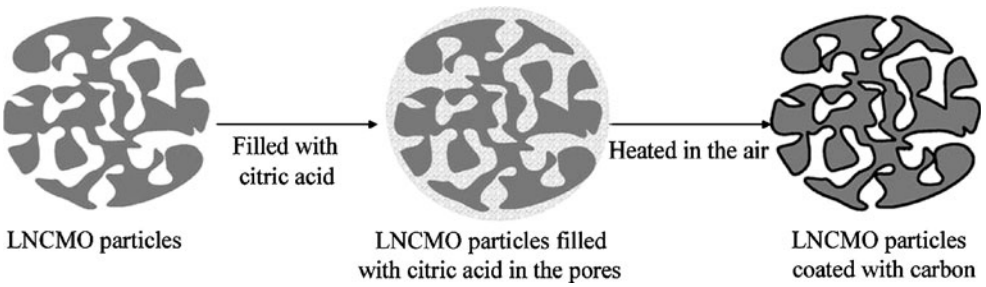

Fig. 2 Illustration of the synthesis of carbon-coated $Li[Ni_{1/3}Co_{1/3}Mn_{1/3}]O_2$

Table 1 Chemical composition, lattice parameters, and tap density for the as-prepared $Li[Ni_{1/3}Co_{1/3}Mn_{1/3}]O_2$

Sample	Composition	*a*(Å)	*c*(Å)	*c*/*a*	I_{003}/I_{104}
LNCMO	$Li_{1.03}Ni_{0.330}Co_{0.332}Mn_{0.338}O_2$	2.859	14.225	4.975	1.22

The electrochemical performance of the powders was evaluated with coin-type cells (CR 2025) with a lithium foil counter electrode and an electrolyte consisting of a 1 M $LiPF_6$ solution in EC/DMC (1:1, *v*/*v*; Zhangjiagang Guotai-Huarong New Chemical Material Co., Ltd.) at room temperature. Microporous polypropylene membrane was used as the separator. The working electrode was prepared from a paste consisting of 80 wt.% active powders, 10 wt.% conductive acetylene black, and 10 wt.% PVDF binder in NMP solvent. The paste was then coated on an aluminum foil, and finally dried under vacuum at 100 °C for 10 h before electrochemical evaluation. The battery was assembled in a glove box (VAC AM-2) filled with pure argon. All the cells were allowed to age for 10 h before testing. The galvanostatic charge–discharge tests were conducted on a LAND CT2001A battery test system with the cut-off voltages of 2.5 and 4.5 V (vs. Li/Li^+) with a charge current density of 32 mA g^{-1} and discharged at different rates.

Results and discussion

Figure 3 showed the XRD patterns of pristine $Li[Ni_{1/3}Co_{1/3}Mn_{1/3}]O_2$ (LNCMO) and carbon-coated $Li[Ni_{1/3}Co_{1/3}Mn_{1/3}]O_2$ (C-LNCMO). The XRD peaks of both samples were narrow, indicating high crystallinity of the products. The chemical composition of LNCMO was determined to be $Li_{1.03}Ni_{0.330}Co_{0.332}Mn_{0.338}O_2$ determined by ICP-OES. All of the peaks could be indexed based on the α-$NaFeO_2$ structure, and no impurity phase was observed. This indicated that the carbon-coating process did not destroy the original layer structure of $Li[Ni_{1/3}Co_{1/3}Mn_{1/3}]O_2$. The cell parameters and the intensity ratio of the main XRD peaks of 003 and 104 were shown in Table 1.

SEM images of LNCMO and C-LNCMO were shown in Fig. 4. It could be seen that the pristine LNCMO was porous and surface of the crystal grain was very smooth apparently (Fig. 4a, b). In contrast, the surface morphology of the carbon-coated $Li[Ni_{1/3}Co_{1/3}Mn_{1/3}]O_2$ was distinctly

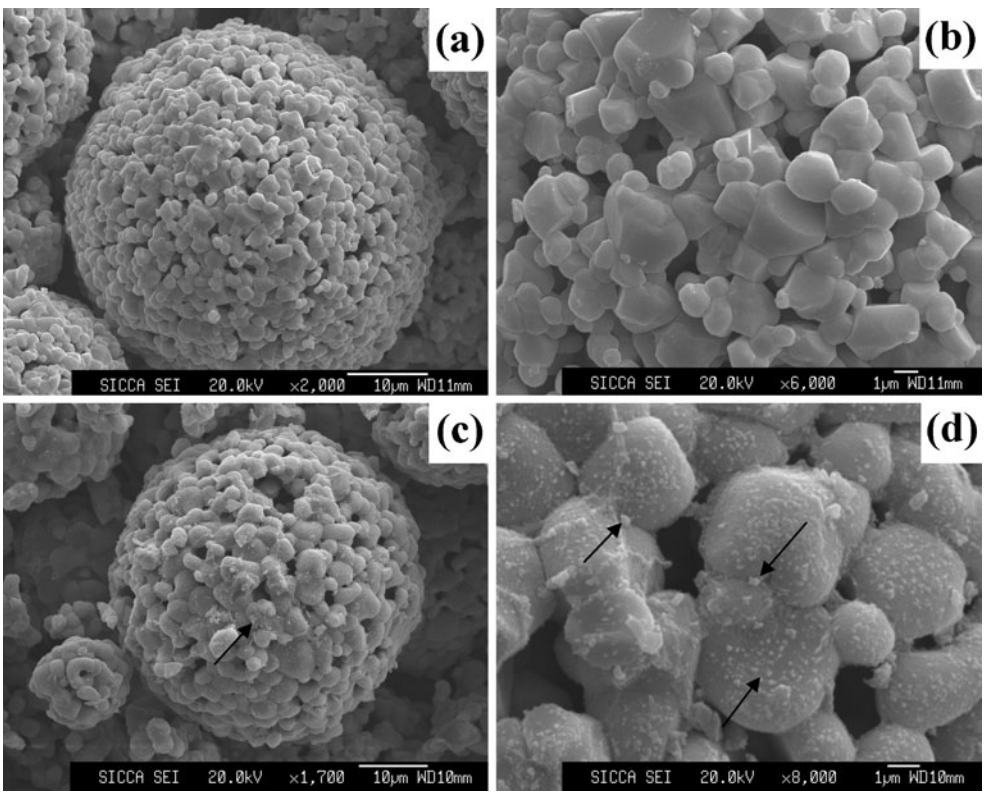

Fig. 4 SEM images of **a**, **b** pristine LNCMO and **c**, **d** C-LNCMO powders

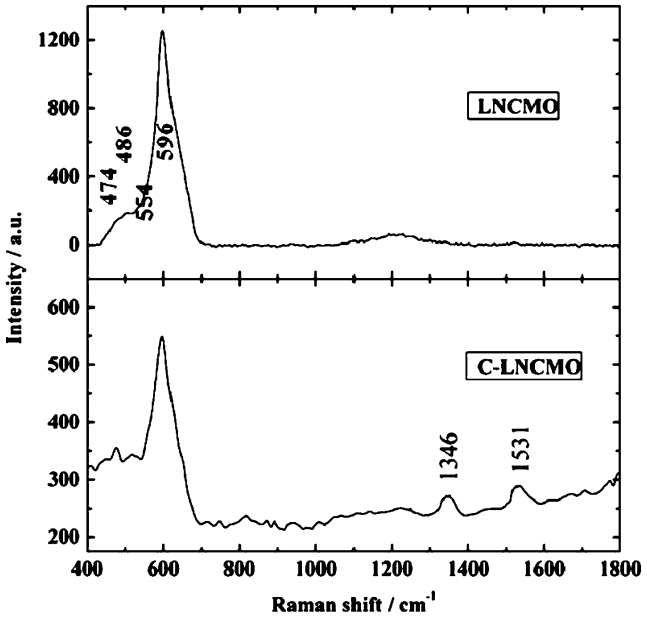

Fig. 5 Raman spectra of the pristine and the carbon-coated $Li[Ni_{1/3}Co_{1/3}Mn_{1/3}]O_2$

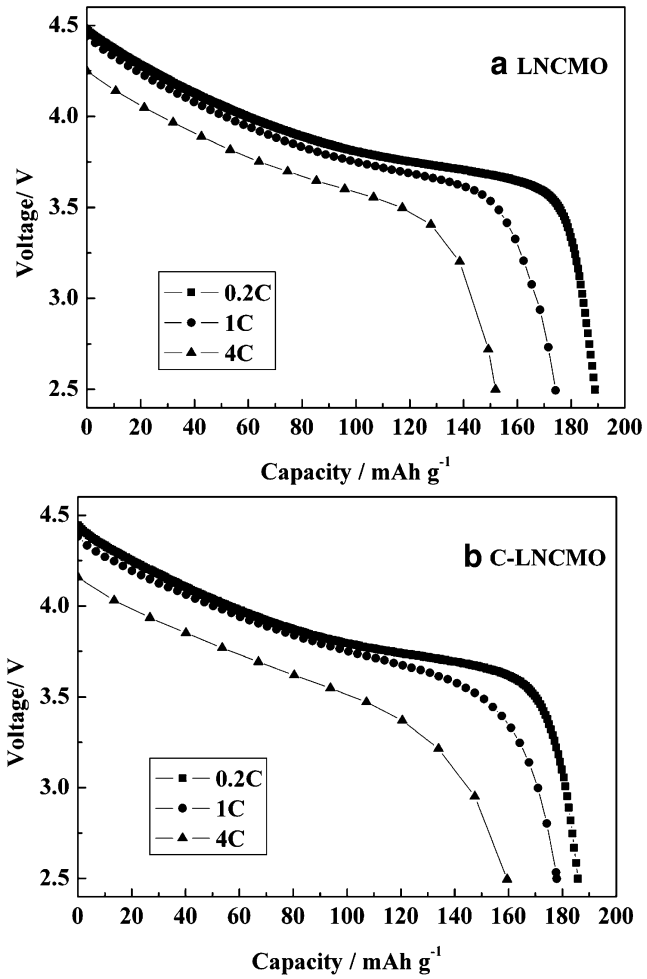

Fig. 6 Rate capability of the **a** pristine LNCMO electrode and **b** C-LNCMO electrode

Table 2 Comparison of rate capabilities between pristine LNCMO electrode and C-LNCMO electrode

Rate (C)	LNCMO		C-LNCMO	
	Discharge capacity ($mAhg^{-1}$)	Ratio (%)	Discharge capacity ($mAhg^{-1}$)	Ratio (%)
0.2	188.9	100.0	185.8	100.0
1	174.2	92.2	177.9	95.7
4	151.9	80.4	159.5	85.8

"Ratio": Discharge capacity of different C rates compared with that of 0.2 C

different from that of the pristine $Li[Ni_{1/3}Co_{1/3}Mn_{1/3}]O_2$. The surface is rough, covered with a layer of homogeneously distributed beads of carbon (Fig. 4c, d, as shown by arrows). BET analysis performed on this material gave an average specific surface area of 3.3 $m^2\ g^{-1}$, which was slightly lower than 3.9 $m^2\ g^{-1}$ obtained from the uncoated material. This might be due to the further growth of the crystal size of LNCMO under 600 °C.

TGA analysis demonstrated ~0.61 wt.% of the carbon content in the C-LNCMO. It was indicated that the carbonization process conducted in air resulted in much lower carbon content than that in inert atmosphere. We also tried to calcine the sample under argon atmosphere to obtain higher carbon content. However, the XRD results of the product under argon indicated that the layer structure of $Li[Ni_{1/3}Co_{1/3}Mn_{1/3}]O_2$ was destroyed due to the reaction with organic precursors.

To investigate the nature of the carbon, Raman microprobe spectroscopy was employed. The Raman spectra of LNCMO and C-LNCMO were shown in Fig. 5. Both spectra had a broad band between 400 and 650 cm^{-1}

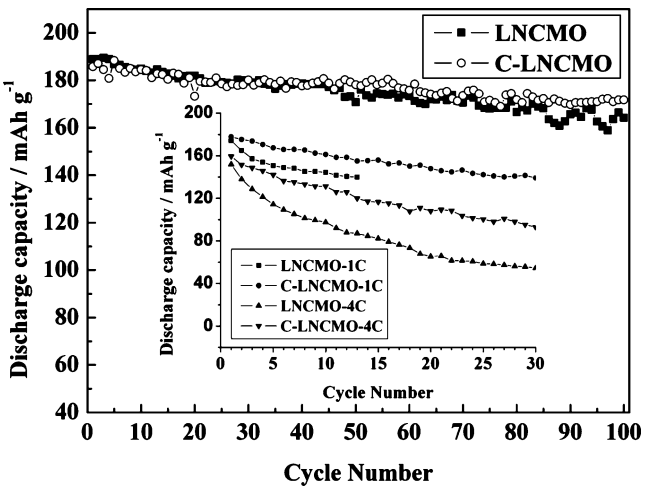

Fig. 7 Cycling performance of the pristine LNCMO electrode and the C-LNCMO electrode cycled between 2.5 and 4.5 V at 0.2 C, 1 C and 4 C (*inset*)

comprising of bands at 474, 554 (Ni–O), 486, 596 (Co–O), and 594 cm^{-1} (Mn–O), respectively, which represented the vibrations within a hexagonal lattice belonging to the same space symmetry group (R3m) [13]. In the case of C-LNCMO, there were two relatively small bands respectively at 1,346 and 1,531 cm^{-1}, which are typical bands of carbon nominated as the D band and G band originated from the amorphous and graphitic forms, respectively. It was therefore indicated that the carbon coated on LNCMO was highly disordered consisted of short-ordered sp^2- and sp^3-coordinated carbon clusters [14, 15].

Figure 6 showed the discharge curves for LNCMO and C-LNCMO at 0.2 C, 1 C, and 4 C rates between 2.5 and 4.5 V, respectively. As seen, the discharge capacity of the LNCMO sample dropped with increasing current density, from 188.9 mAh g^{-1} at 0.2 C to 174.2 mAh g^{-1} at 1 C and 151.9 mAh g^{-1} at 4 C. This result was comparable or even superior to that of the popular hydroxide co-precipitation method, which might be attributed to the particular porous morphology formed by the spray drying process that was favorable for the charge transfer during the deintercalation and intercalation cycling [12]. The rate capability was improved further by carbon-coating. The C-LNCMO sample presented a capacity of 159.5 mAh g^{-1} at current density of 4 C, corresponding to 85.8% of its capacity at 0.2 C. The electrochemical properties summarized in Table 2 confirmed the positive effect of carbon-coating in improving the rate capability of $Li[Ni_{1/3}Co_{1/3}Mn_{1/3}]O_2$ which would be related to the increased electronic conductivity between the primary particles.

Comparison of cycling performances between carbon-coated $Li[Ni_{1/3}Co_{1/3}Mn_{1/3}]O_2$ and the pristine one was shown in Fig. 7. The initial discharge capacity of LNCMO at 0.2 C was about 188.9 mAh g^{-1}. Compared with the pristine one, carbon-coated C-LNCMO exhibited comparable discharge capacity, i.e., 185.8 mAh g^{-1}. After the 100th cycling at 0.2 C, the cell delivered about 86.9% and 92.4% of the initial discharge capacity for the pristine LNCMO and carbon-coated C-LNCMO, respectively. Especially C-LNCMO displayed distinctly lower fading rate than LNCMO at higher rate (inset in Fig. 7), though both materials showed similar capacities. Similar effect was also found in carbon-coated $LiNi_{0.5}Mn_{0.5}O_2$ material reported by Goodenough's group [11]. The capacity fading of $Li[Ni_{1/3}Co_{1/3}Mn_{1/3}]O_2$ was normally ascribed to the polarization effect [16], therefore it became more serious at higher current densities. After carbon-coating, the electronic conductivity was increased, which reduced cell polarization and prevented the evolution of oxygen from the cathodes at the end of charge, thus suppressed the capacity fade especially at high rates.

Conclusions

The carbon-coated $Li[Ni_{1/3}Co_{1/3}Mn_{1/3}]O_2$ was synthesized from the porous $Li[Ni_{1/3}Co_{1/3}Mn_{1/3}]O_2$ and citric acid. The carbonization process conducted in air maintained the original layer structure of $Li[Ni_{1/3}Co_{1/3}Mn_{1/3}]O_2$ and resulted in highly disordered carbon coated on LNCMO. The electrochemical results showed that both cycling performance and rate capability were improved by the carbon-coating. It is believed that the enhanced cycling properties by the carbon-coating are attributed to the increased electronic conductivity because the carbon distributed among the surface and in the pores of spherical powders favored the transference of electrons among the particles and lead to the reduction of cell polarization, thus prevented the evolution of oxygen from the cathodes at high charge voltage, and improved the cycling performance at high rate.

Acknowledgments This work was financially supported by NSFC Project No. 20333040 and 50672114, 863 Project of China No. 2006AA03Z232, and 973 Project of China No. 2007CB209700, as well as Research Projects from the Science and Technology Commission of Shanghai Municipality No. 08DZ2210900.

References

1. Ohzuku T, Makimura Y (2001) Chem Lett 642–643
2. Yabuuchi N, Ohzuku T (2003) J Power Sources 119–121:171–174
3. Belharouak I, Sun YK, Liu J, Amine K (2003) J Power Sources 123:247–252
4. Kim GH, Kim JH, Myung ST, Yoon CS, Sun YK (2005) J Electrochem Soc 152:A1707–A1713
5. Li J, He X, Zhao R, Wan C, Jiang C, Xia D, Zhang S (2006) J Power Sources 158:524
6. Kim GH, Kim MH, Myung ST, Sun YK (2005) J Power Sources 146:602–605
7. Kim GH, Myung ST, Kim HS, Sun YK (2006) Electrochim Acta 51:2447–2453
8. Lin B, Wen ZY, Gu ZH, Xu XX (2007) J Power Sources 174:544–547
9. Jang SB, Kang SH, Amine K, Bae YC, Sun YK (2005) Electrochim Acta 50:4168–4173
10. Huang H, Yin SC, Nazar LF (2001) Electrochem Solid-State Lett 4:A170–A172
11. Cushing BL, Goodenough JB (2002) Solid State Sci 4:1487–1493
12. Lin B, Wen ZY, Gu ZH, Huang SH (2008) J Power Sources 175:564–569
13. Kerlau M, Marcinek M, Srinivasan V, Kostecki RM (2007) Electrochim Acta 52:5422–5429
14. Doeff MM, Hu YQ, McLarnon F, Kostecki R (2003) Electrochem Solid-State Lett 6:A207–A209
15. Hsu KF, Tsay SY, Hwang BJ (2005) J Power Sources 146:529–533
16. Shaju KM, Subba Rao GV, Chowdari BVR (2002) Electrochim Acta 48:145–151